Slow Dynamics and Aging in Spin Glasses

Eric Vincent, Jacques Hammann, Miguel Ocio, Jean-Philippe Bouchaud and Leticia F. Cugliandolo

Service de Physique de l'Etat Condensé, CEA Saclay, 91191 Gif-sur-Yvette Cedex, France

1 Introduction

A crucial feature of the behavior of *real* spin glasses is the existence of *extremely slow relaxational processes*. Any field change causes a very long-lasting relaxation of the magnetization and, the response to an ac excitation is noticeably delayed. In addition, the characteristics of this slow dynamics evolve during the time spent in the spin-glass phase: the systems *age*.

Aging effects in real spin glasses have been layed down by experiments [1, 2, 3] at a time where there was already an intense theoretical activity on the equilibrium properties of mean-field spin-glass models [4]. Experimentalists started comprehensive studies of the non-equilibrium dynamics, which happened to bring very instructive surprises, while in the meantime theoreticians developed extremely sophisticated methods for progressing towards solutions of the equilibrium mean-field problem, thence inventing incentive tools for the statistical mechanics of disordered systems.

This early epoch was not the time for the most productive dialogue between both parts. The situation is very different now; experiment and theory have had, during these last years, a fruitful interplay. On the one hand, the problem of the non-equilibrium dynamics has now been theoretically addressed from very different points of view; scaling theories of domain growth [5, 6, 7, 8], a phase-space approach motivated by the Parisi solution to mean-field models [9], a percolation like picture in phase space [10], random walks in phase space [11, 12, 13], mean-field treatments of some simplified situations [14, 15], are now providing us with various (and sometimes contradictory) lightings of the experimental results, together with impulsing a thrilling debate on the sound nature of the spin-glass phase. On the other hand, more and more complex experimental procedures [16, 17, 18] have been conceived with the aim of evidencing the materialization of some abstract theoretical notions, like *e.g.* the ultrametric organization of states or the chaotic dependence of the spin-spin correlation function on temperature.

In this paper, we recall some important experimental features of the spin glass dynamics. Since we intend to picture some aspects of the present state of

the dialogue between experimentalists and theoreticians, we give a detailed description of several ways of scaling the data and of the connection between these scalings and the theoretical predictions. We obviously give up any pretention of giving an exhaustive comparison of theory and experiment; we mainly focus here on a perspective of spin glasses which proceeds from mean-field results [14] (abundant discussions of the scaling theories can be found in the literature of the past few years). In several occasions, we use as a guideline for the description of the experimental results a probabilistic model that views aging as a thermally activated random walk in a set of traps with a wide distribution of trapping times [12].

The slow dynamics of spin glasses - and, as well, of structural glasses [19] and other disordered systems - has been often interpreted in terms of thermal activation over barriers. One likes to think of a complex free-energy landscape (due to frustration) with peaks and valleys of all sizes. This picture has been extensively used in the litterature; Refs. [9, 11, 12, 13, 18, 20] are examples of different ways of drawing conclusions from it. In fact, the experiments never directly probe free-energy valleys or mountains, but rather give access to relaxation rates at various time scales, which may then be interpreted in terms of thermal activation over free-energy barriers [18].

However, when trying to describe the slow dynamics and aging of real spin glasses with a "phase-space" viewpoint, it is worth noticing that phase-space is infinite dimensional irrespectively of the finite or infinite dimensionality of real space. The geometrical properties of the infinite-dimensional phase space may put at work a different (non-Arrhenius) mechanism for slow dynamics that leads to slowing-down and aging even in the absence of metastable states [21]. The particle point in phase space, representing the system configuration, slowly decays through almost flat regions. This mechanism seems to be the one acting in the dynamics of mean-field spin-glass models (with a single aging correlation scale) [14] as well as in domain growth. In these models one does not see neither a severe change of behavior when approaching the zero-temperature limit nor rapid barrier-crossings from trap to trap in numerical simulations [15, 21].

We describe below some mean-field predictions which compare rather well with the experiments at constant temperature. Whether one can describe more subtle experimental results such as temperature variation dependences, etc. with mean-field models and/or with the above non-Arrhenius phase space geometrical description is still an open question. The rather good agreement at constant temperature suggests that the phase-space dynamical mechanism at the base of the dynamics of spin glasses may be a combination of rapid activated processes and slow decay through flat regions [14, 21, 22]. We might thence be led to revise our "common sense understanding" of the slow dynamics in disordered systems.

2 Experimental Evidence for Non-Stationary Dynamics

2.1 Magnetization Relaxation in Response to a Field Change

In a measurement of the relaxation of the "thermo-remanent magnetization" (TRM), the system is cooled in a small field from above T_g down to some $T_0 < T_g$; it then "waits" in the field at T_0 during a time t_w, after which the field is cut, and the subsequent decrease of the TRM from the field-cooled (FC) value is recorded as a function of t. Following an "immediate fall-off" of the magnetization (depending on the sample and on temperature, of the order of 50 to 90 %), a slow logarithmic-like relaxation takes place; it is believed to head towards zero, although never reaching an end at laboratory time scales.

These endless-like relaxation processes and, more crucially, the existence of "aging" phenomena [1, 2, 3] are a salient feature of spin-glass dynamics: for different values of the waiting time t_w, different TRM-decay curves are obtained, as is evidenced in Fig. 1.a.

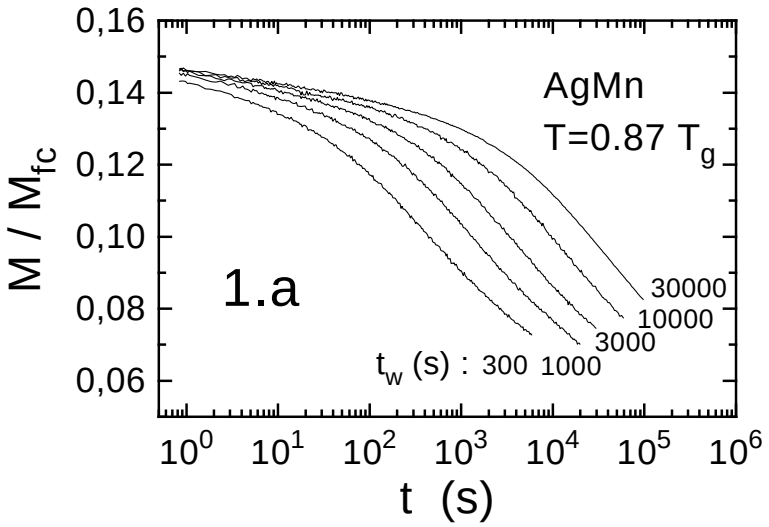

Fig. 1. a. Thermo-remanent magnetization M, normalized by the field-cooled value M_{fc}, *vs.* $t(s)$ ($\log_{10}$ scale) for the $Ag : Mn_{2.6\%}$ sample, at $T = 9K = 0.87T_g$. The sample has been cooled in a 0.1 Oe field from above $T_g = 10.4K$ to 9K; after waiting t_w, the field has been cut at $t = 0$, and the decaying magnetization recorded.

The dynamics depends on two independent time-scales, t ("observation time") and t_w ("waiting time"). This dynamics is *non-stationary*: the response at $t+t_w$ to an excitation at t_w depends on $t + t_w$ and t_w, and not only on t (breakdown of time-translational invariance). Qualitatively, one can see in Fig. 1.a that the

longer the waiting time before cutting the field, the slower the overall response; the initial fall-off is smaller, the relaxation curve shows a slower decrease, the system has become "stiffer". Such aging phenomena have been early identified in the mechanical properties of glassy polymers [1] [23]; the slow strain following the application of a stress has been recognized to depend on the time spent in the glassy phase.

In spin glasses, the aging phenomena have initially been explored using the mirror experimental procedure of the TRM [1], in which the sample is cooled in zero-field, and after t_w a small field is applied. As far as the field remains low enough (usually, in the range 0.1-10 Oe), both procedures are equivalent; the relaxation of this "zero-field cooled magnetization" (ZFC) follows the same t *and* t_w dependence as the relaxation of the TRM [24, 25]. More precisely, it has been shown in [24] that, for all t, t_w values (*i.e.* all along the measured relaxations for various t_w), the sum of the ZFC-magnetization plus the TRM equals the field-cooled value. This is simply *linearity* in the response, since this experimental result shows that *the sum of the responses to different excitations* is equal to *the response to the sum of both excitations* (the response to a constant field being the field-cooled magnetization). That linearity holds for all t, t_w tells us that the presence of the (sufficiently small) field does not influence the aging process: waiting t_w in zero field and then applying a field during t (ZFC case) is equivalent, for the dynamics, to applying a field during t_w and then waiting t in zero field (TRM case). The only role played by the field in this context is to reveal the dynamic properties of the system. A recent study of the effect on the dynamics of increasing field values can be found in [20, 26, 27].

In the semi-log plot of Fig. 1.a, each curve shows an inflection point, and one first quantitative estimate of the t_w-effect on the relaxation is that this inflection point is located around $\log t \simeq \log t_w$. This fact has been noticed and given a physical meaning by Lundgren *et al.* [1]. The relaxations are slower than exponential; they do not correspond to a single characteristic response time τ, but are likely to be parametrized with the help of a wide distribution $g_{t_w}(\tau)$, which is defined hereby:

$$m_{t_w}(t) \equiv \frac{M(t+t_w, t_w)}{M_{fc}} = \int_{\tau_0}^{\infty} g_{t_w}(\tau) \exp(-\frac{t}{\tau}) d\tau \tag{1}$$

where $\tau_0 \simeq 10^{-12} sec$ is a microscopic attempt time. $M(t+t_w, t_w)$ is the ZFC or TRM, depending on the experiment, and $M_{fc}(t+t_w)$ is the field-cooled value at time $t+t_w$. In the figures we abbreviate $M(t+t_w, t_w)/M_{fc}(t+t_w) = M/M_{fc}$. Lundgren *et al.* have pointed out that taking the derivative of (1) with respect to $\log t$ gives access to the distribution $g_{t_w}(\tau)$, since

$$\frac{dm_{t_w}(t)}{d\log t} = -\int_{\tau_0}^{\infty} g_{t_w}(\tau) \frac{t}{\tau} \exp(-\frac{t}{\tau}) d\tau \approx g_{t_w}(\tau = t) \ , \tag{2}$$

[1] A wide class of materials like *e.g.* PVC, PS, Epoxy, or even bitumen, Wood's metal, amorphous sugar and cheese [23].

a rough approximation reflecting the sharp character of $\frac{t}{\tau}\exp(-\frac{t}{\tau})$ around $t=\tau$ (to be considered on a logarithmic scale, which is actually the scale which is suggested by the measurements). The plot of the relaxation derivatives shows bell-like shapes, with a broad maximum around $\log t = \log t_w$, and pictures $g_{t_w}(\tau)$ for various t_w [1]. Thus, in a first approximation, the aging phenomenon can be described as a *logarithmic shift towards longer times* of a wide spectrum of response times [2]. This shift is of the order of $\log t_w$, and therefore suggests that the dynamics be the same as a function of t/t_w.

Let us call "full aging" the pure t/t_w scaling, that is not far from being the correct one, as seen in Fig. 1.b where the data from Fig. 1.a is presented versus t/t_w. Most of the t_w-effect has been accounted for, though some systematic departures remain, and are worth being discussed (see Sect. 4.2).

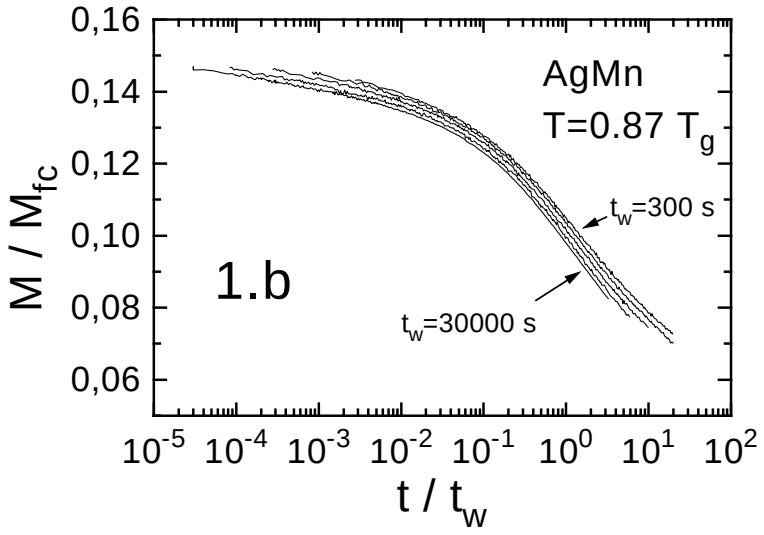

Fig. 1. b. Same TRM data as in Fig. 1a, presented as a function of t/t_w.

2.2 Ac susceptibility

The approximate t/t_w scaling of the TRM (or ZFC) curves is sufficient for a description of aging effects in ac experiments, where the in-phase and out-of-phase components of the response to a small ac excitation field at a frequency

[2] Indeed, the spin-glass properties do not exactly depend on t_w, but rather on the *total* elapsed time $t_w + t$ (Sect. 4.2); they are evolving during the TRM measurement itself [3, 28]. The physical interpretation [1] of $g_{t_w}(\tau)$ therefore remains approximate.

ω are measured. Aging is more visible (in relative value) in the out-of-phase component χ'' of the magnetic susceptibility, which represents dissipation. The *observation time*, corresponding to t in TRM experiments, is here constant, equal to $1/\omega$. When the sample is cooled from above T_g down to $T_0 < T_g$, the susceptibility does not immediately reach an equilibrium value, but shows a slow relaxation as time goes on. We denote t_a ("age") this time elapsed from the quench into the spin-glass phase; in the TRM experiment, the equivalent age is $t + t_w = t_a$. The *non-stationary* character of the dynamics, which appears in the TRM measurements as a dependence on the two independent time scales t and t_w, shows up in ac experiments as a dependence of χ" on the two variables ω *and* t_a. This is clear in Fig. 2 where χ" at various (low) frequencies ω is plotted as a function of ωt_a; applying a vertical shift, the curves can all be merged with respect to this reduced variable, which is equivalent to t/t_w in TRM experiments.

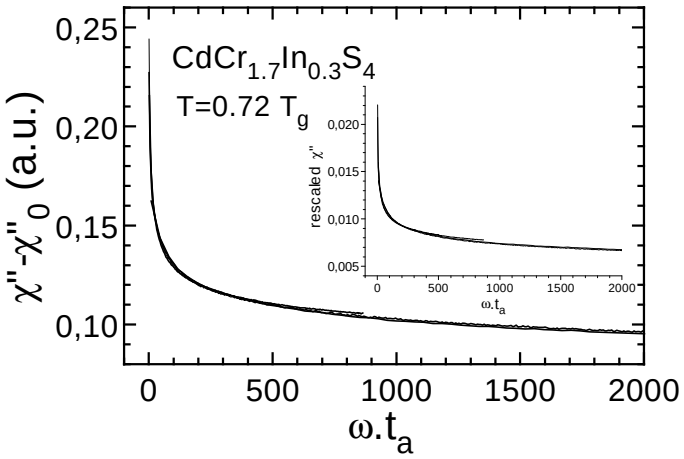

Fig. 2. Out of phase susceptibility $\chi(\omega, t_a)$ *vs.* $\omega\, t_a$ for the insulating $CdCr_{1.7}In_{0.3}S_4$ sample. The four curves, corresponding to $\omega = 0.01, 0.03, 0.1, 1.\ Hz$, have been vertically shifted (see text). t_a is the total time elapsed from the quench (age). The inset shows a scaling of the same data which follows from mean-field results (see Sect. 3.2).

Thus, the approximate t/t_w scaling obtained from TRM and ZFC experiments can be fairly well transposed to an $\omega.t_a$ scaling of the ac susceptibility $\chi"(\omega.t_a)$. The vertical shift corresponds to accounting for the various "equilibrium values" $(\chi"_{eq}(\omega) = \lim \chi"(\omega, t_a \to \infty))$ at different frequencies. In Fig. 2, for technical reasons, the zero of the scale has not been measured and the shift is arbitrary. As an example of the relative orders of magnitude, let us mention that, at $\omega = 0.01Hz$, the amount of the relaxing part is roughly equal to the equilibrium value; for χ' in the same conditions, it would be of the order of 10% of the equilibrium value. The frequency-dependence of $\chi"_{eq}$ has been determined

in other studies [25, 28]; it can be represented by a power law with a very small exponent (or else a power law of a logarithm)

$$\chi"_{eq}(\omega) \propto \omega^{\alpha} \ , \tag{3}$$

where α increases in the range $0.01 - 0.1$ when approaching T_g from below. This is valid in the $10^{-2} - 10^{5} Hz$ range which has been explored, and has been measured rather in insulating than in intermetallic spin glasses (due to eddy currents in metals). Both classes of samples have been found to present the same general spin-glass behavior [3, 28]. The $\omega.t_a$ scaling indicates that the smaller the frequency, the longer the time t_a during which a significant relaxation, characteristic of aging effects, can be found. Therefore, at higher frequencies ($\omega \geq 10Hz$) aging disappears very rapidly, yielding almost instantaneously a stable value $\chi"_{eq}(\omega)$; conversely, at lower frequencies, the determination of $\chi"_{eq}(\omega)$ becomes problematic, implying measurements over tens of hours or days.

2.3 Time Regimes in ac and dc Experiments

Let us summarize the conditions for observing either stationary or non-stationary (aging) dynamics in ac($\chi"$) and dc (TRM or ZFC) measurements. We can define two distinct time regimes, which apply to both experiments.

- For $\omega.t_a \to \infty$, "equilibrium dynamics" is recovered in ac experiments, in the sense that only one time scale is needed: the dynamics is then *stationary*. This time regime corresponds, for TRM's, to $(t_w + t)/t = t_a/t \gg 1$ or equivalently $t \ll t_w$, that is the very beginning of the TRM-decay curves.

- If ωt_a is comparable to t_a ($\omega t_a = O(1)$) in the χ'' experiments and, equivalently, t is comparable to t_w in the TRM experiments, one observes non-stationary dynamics.
  The χ'' measurements are limited to $\omega t_a > 1$ since $\omega.t_a < 1$ cannot be experimentally realized (the harmonic response is not defined at times shorter than one period). Hence, with χ'' we can only explore the beginning of the aging regime.
  In contrast, aging is predominant in TRM-measurements over the largest part of the accessible time scale since, for TRM's, $(\omega.t_a) \equiv t_a/t = (t_w + t)/t$ becomes rapidly close to 1 as the observation time t elapses. Measuring the TRM decay we have access to a larger time-window in the aging regime.
  Therefore, aging in χ'' can only be compared with the TRM decay at the beginning of the aging regime – that we call early epochs (also called "quasi-stationary regime" in [28]). This might explain why a full aging scaling seems to apply better to $\chi"$ results than to the TRM (see Fig. 1.b and 2).

3 Aging Theories for Old Results

3.1 Scaling theories

The different time scales in which *stationary* and *non-stationary* dynamics are occurring are likely to be mapped onto length scales in the real space of spins. When approaching T_g from above, the onset of a critical regime has been characterized by the diverging behavior of the characteristic time in ac experiments and of the non-linear susceptibility in dc studies, [29]. A thermodynamic phase transition would imply the divergence of a characteristic correlation length ξ when $T \to T_g$. In this equilibrium picture the spin-glass phase is believed to be an ensemble of randomly oriented spins, which are frozen due to infinite-range correlations corresponding to a long-distance "order".

However, aging shows that indeed equilibrium has not been established when crossing T_g. In several "scaling theories" [5, 6, 7, 8] of non-equilibrium phenomena in spin glasses, the spin correlations are considered to be limited to some *finite* range $\xi(t)$ (out-of-equilibrium situation); as time elapses, spin rearrangements yield a slow (due to frustration) extension of equilibrium correlations, towards the equilibrium situation of infinite range ($t \to \infty, \xi(t) \to \infty$). An ac experiment at frequency ω, as well as a TRM or ZFC relaxation at time t, can be viewed as probing the spin-glass excitations at a given length scale L which should be an increasing function of the *characteristic probe time* $1/\omega$ for χ" and t for TRM. In the "droplet model" by Fisher and Huse [6], one has $L \propto \log^{1/\psi} t$ ($\psi \leq d-1$), and in the "domain model" by Koper and Hilhorst [7] $L \propto t^{p/d}$ ($p \sim 0.5$). These theories do not aim at a microscopic description at the scale of spins, but make this mapping of *time* onto *length* scales quantitative, in terms of scaling laws. At least qualitatively, these models provide us with a convenient picture of aging phenomena, which is the following. For short probe times compared to the age ($\omega.t_a \gg 1$, or $t/t_w \ll 1$), short-ranged excitations are involved ($L \ll \xi(t)$), and the increase with time of $\xi(t)$ does not affect the dynamics, which is found to be stationary (no aging). Conversely, for longer probe times compared to the age ($\omega.t_a \sim 1$, or $t \geq t_w$), the characteristic length of the relevant excitations is of the same order of magnitude as $\xi(t)$, which is increasing due to aging, and the dynamic properties are strongly affected by aging (non-stationary dynamics).

The accurate quantitative agreement with the data is still to be discussed (see *e.g.* Ref. [13]). Some critical remarks to the simple scaling approaches, which rise up in view of other results (T-variation experiments), are discussed in Sect. 5.1.

3.2 Non-Equilibrium Dynamics in Microscopic Theories

The Models. The classical "realistic" microscopic model of spin glasses is the 3-D Edwards-Anderson (3DEA) model [30]

$$H = -\sum_{\langle i,j \rangle} J_{ij} S_i S_j \ , \tag{4}$$

where J_{ij} are Gaussian or bimodal random variables, S_i are Ising spins and $\langle i, j \rangle$ represents a sum over first neighbours on a cubic 3D lattice. It is very difficult to obtain analytical results for the statics or the dynamics of 3DEA, in consequence, even after more than 20 years of research on the field of spin glasses, very few results are available. A lot of efforts have been devoted to the numerical study mainly of the equilibrium properties of the 3DEA. Again, the situation is still pretty unclear: basic questions as to the existence of a thermodynamic phase transition are still not answered [31].

The standard mean-field extension of the 3DEA model is due to Sherrington and Kirkpatrick (SK) [32] and corresponds to the same interactions as in (4) but with the sum extended to hold over all pairs of spins in the system. The study of the SK model - and of some other related mean-field models - had for a long time been confined to the search for equilibrium properties [4].

Numerical Simulations of Out-of-Equilibrum Phenomena. One may wonder whether aging, which did at first sight appear as some imperfection of the experiments, is really intrinsic to the Hamiltonian (4). We now know that the answer is yes. Only recently, attention has been paid to the study of the out of equilibrium dynamics of microscopic spin-glass models. Andersson *et al.* [33] and Rieger [34] reproduced in a numerical simulation the procedure of, *e.g.*, the TRM experience using the 3DEA model. The results show that it captures the main features of real spin glasses: both slow dynamics and aging effects. Later, numerical simulations of the large D "hypercubic" spin-glass cell in real space showed that also this model, that is expected to reproduce the SK model, when $D \to \infty$, captures the main characteristics of aging [35], thus confirming the previous analytical results that we describe in the following paragraphs.

Analytical Approach: Formulation and Definitions. Again, it only happened recently that *analytical* developments evidenced aging effects in mean-field spin-glass models [14], showing that these simplified models can describe, at least qualitatively, the phenomenology of real spin glasses. The idea in the case of mean-field spin-glass models is just to try to solve the *exact* dynamical equations derived for N, the number of dynamical variables in the model, tending to infinity. These equations are well-defined, have a unique solution and, in the absence of a magnetic field, only involve the correlation and the response functions (see Eqs.(5),(10) below for their definitions). The initial condition is chosen to be random so as to mimic the initial configuration just after the quench in the experimental situation. One then considers the large-time limits, but only after having already taken the thermodynamic limit $N \to \infty$ to obtain the asymptotic behavior of the solution.

It is important to notice that in this approach it is not necessary to assume *a priori* any particular structure of phase space - typically to say that there are many metastable states due to frustration separated by high barriers - to obtain the dynamical behavior of the problem. The solution can *a posteriori* be given a geometrical interpretation [12, 13, 21, 22].

The solution shows that the equations are self-consistently solved in the large-time limit by an *aging* solution. The reason why these equations can be solved is the *weak long-term memory* of the system [14]. The results fall into the *weak-ergodicity breaking scenario* previously proposed in [12, 13] within the trap model (see Sect. 3.3 below). When looking at the large-time dynamics of the system, the weak long-term memory property allows us to neglect the contribution of any finite time-interval after the quenching time. The system forgets what happens in "finite" time intervals with respect to the "infinite" observation time. It keeps, however, an averaged memory of its history. The weak-ergodicity breaking scenario tells us that the evolution of the system continues forever; the dynamics slows down as time elapses but the system is never completely stopped in its evolution. The waiting-time t_w gives us an idea of the age of the system.

In the following we shall be a bit more technical and describe the main features of the formalism and the solution.

The auto-correlation function is defined as

$$C(t+t_w,t_w) \equiv \frac{1}{N}\sum_{i=1}^{N} \overline{\langle s_i(t+t_w)s_i(t_w)\rangle}\ , \tag{5}$$

with the overline representing a mean over different realizations of the disorder and $\langle\,\rangle$ an average over different realizations of the thermal noise. We then define

$$C_F(t) \equiv \lim_{t_w\to\infty} C(t+t_w,t_w) \qquad C_F(0)=1 \qquad \lim_{t\to\infty} C_F(t) = q_{EA}\quad . \tag{6}$$

This allows us to separate the auto-correlation into two *additive* parts, a *stationary* term and an *aging* term C_A [14, 13]:

$$C(t+t_w,t_w) = C_F(t) - q_{EA} + C_A(t+t_w,t_w)\quad . \tag{7}$$

In the absence of a magnetic field, the weak ergodicity breaking scenario [12, 13, 14] implies

$$\lim_{t\to\infty} C(t+t_w,t_w) = 0 \qquad \forall \text{ fixed } t_w\ , \tag{8}$$

thus

$$\begin{aligned} \lim_{t\to\infty}\lim_{tw\to\infty} C_A(t+t_w,t_w) &= q_{EA} \\ \lim_{t\to\infty} C_A(t+t_w,t_w) &= 0\ . \end{aligned} \tag{9}$$

It will turn out that the two scales corresponding to these two limits are well-separated for mean-field models, in the sense that in the time-regime where C_F varies then C_A stays constant, and *viceversa*. In other words, one can think of q_{EA} as a value of the correlation separating different "correlation-scales", $C > q_{EA}$ and $C < q_{EA}$: when $t \ll t_w$, $C > q_{EA}$ and we have stationary dynamics, while when $t \gg t_w$, $C < q_{EA}$ and we have non-stationary dynamics and aging just as described in Sect. 2.3 for the general features of aging in spin glasses. [3]

[3] In some numerical works, the form $C(t+t_w,t_w) = t^{-x(T)}\,\Phi(t/t_w)$ has been often used to scale the data for all times t ([34, 35, 36, 37], see also [28] for a related

In the same way, the response function can be equivalently separated into a *stationary* and a *non-stationary* term

$$R(t+t_w,t_w) \equiv \frac{1}{N}\sum_{i=1}^{N} \left.\overline{\frac{\partial\langle s_i(t+t_w)\rangle}{\delta h_i(t_w)}}\right|_{h=0} = R_F(t) + R_A(t+t_w,t_w)\ . \qquad (10)$$

with

$$R_F(t) \equiv \lim_{tw\to\infty\ C(t+t_w,t_w)>q_{EA}} R(t+t_w,t_w) \quad and \qquad (11)$$

$$R_A(t+t_w,t_w) \equiv \lim_{tw\to\infty\ C(t+t_w,t_w)<q_{EA}} R(t+t_w,t_w) \quad . \qquad (12)$$

$R_F(t)$ satisfies the fluctuation-dissipation theorem (FDT) and $R_A(t+t_w,t_w)$ satisfies a generalized FDT [14]

$$R_F(t) = -\frac{1}{T}\frac{dC_F(t)}{dt} \qquad R_A(t+t_w,t_w) = \frac{X[C_A(t+t_w,t_w)]}{T}\ \frac{\partial C_A(t+t_w,t')}{\partial t'}|_{t'=tw}\ , \qquad (13)$$

with $0 \le X[C_A] \le 1$ a monotonically increasing function of $0 \le C_A \le q_{EA}$. ($X = 1$ corresponds to the usual FDT.)

With these definitions one can solve the asymptotic (large t_w) dynamics of several mean-field disordered models [14, 15, 38, 39, 57].

Analytical Approach: Stationary Regime. For all these models, when t is large, the *stationary* part of the correlation function $C_F(t)$ decays with a power law

$$C_F(t) \sim q_{EA} + c_\alpha \left(\frac{\tau_0}{t}\right)^\alpha\ , \qquad (14)$$

where τ_0 is a microscopic time-scale and α has precisely the same meaning as the exponent in (3), describing the frequency dependence of the equilibrium out of phase susceptibility.

The temperature dependence of α depends on the model. For models [4] such as the p-spin spherical spin glass [40, 39] or the model of a particle moving in an infinite-dimensional random potential [41, 39], $\alpha = 1/2$ at $T = 0$ and

discussion of the experimental data). It should be remarked that, though at first glance this scaling seems to be similar to the one following from the WEB scenario, it implies quite a different conclusion for the global behavior of the system. Note that if one takes the limit $\lim_{t\to\infty}\lim_{t_w\to\infty}$, that corresponds to exploring the *end of the stationary dynamics*, Eqs.(6) yield $\lim_{t\to\infty}\lim_{t_w\to\infty} C(t+t_w,t_w) = q_{EA}$, while $\lim_{t\to\infty}\lim_{t_w\to\infty} t^{-x(T)}\,\Phi(t/t_w) = \Phi(0)\ \lim_{t\to\infty} t^{-x(T)} = 0$. The stationary dynamics *and* the fact that the correlation decays to q_{EA} at the end of this time-regime, have a very clear geometrical interpretation [13, 14, 21].

[4] Though the aim of Refs. [40, 41] was to study the equilibrium dynamics à la Sompolinsky [42] - a different situation from the out of equilibrium occuring in experiments - the calculation of the exponent α obtained in these works applies to the experimental case when adequately reinterpreted [14]. Let us also note that the in this paper the α and β exponents are exchanged with respect to Refs. [39].

it decreases when increasing the temperature. For the SK model, conversely, $\alpha = 1/2$ at $T = T_c$ and it decreases when decreasing the temperature [43]. Finally, for the mixed ($p = 2 + 4$) spherical model introduced in Ref. [44], α has a non-monotonic dependence on T; $\alpha(T = 0) = \alpha(T_c) = 1/2$. The value of the exponent α measured experimentally follows the tendency of the one holding for SK and the mixed ($p = 2 + 4$) spherical models close to the critical temperature, though the value of α from the experiments is considerably smaller ($\alpha \leq 0.1$ *vs* $\alpha \sim 0.5$).

Analytical Approach: Non-Stationary Regime. Following then very general requirements, it has been argued in Ref. [14, 15], and explicitely checked on several pure and disordered models, that in the large-time limit only two situations with different dynamical behavior seem to exist:

– On the one hand, there are models with only one time-scale – or equivalently, correlation-scale – apart from the stationary one. C_A scales as in a domain growth process within the non-stationary time-scale, in the sense that:

$$C_A(t_w + t, t_w) = \jmath^{-1}\left(\frac{h(t + t_w)}{h(t_w)}\right) \tag{15}$$

with $h(t)$ a monotonically increasing function – analogous to the domain length $L(t)$. $\jmath^{-1}(u)$ is a function characterized by another exponent which we call here $(1 - x)$ (and has been called β in [39] and α in [45]). Close to $u = 1$, *i.e.* for the early epochs of the aging regime, $\jmath^{-1}$ reads

$$\jmath^{-1}(u) \sim q_{EA} - c(1 - u)^{1-x} , \tag{16}$$

c is a constant and $x < 1$ implying that $\jmath^{-1}$ is non-analytical in the neighbourhood of $u = 1$ (see (35) below).
In this case, the FDT-violating factor $X[C_A]$ is a constant $X < 1$. These models, when treated statically with the replica trick, are solved by a *one step replica symmetry breaking* ansatz [4]. An example is the p-spin spherical model [46]. We call them "single-scale models".
Certainly the functions h and $\jmath^{-1}$ do depend on the specific model. At the mean-field level we have succeeded in obtaining $\jmath^{-1}$ and X for several models. However, surprisingly, there are for the moment no analytical results available for the scaling function $h(t)$ [5]. The simplest possibility is that $h(t)$ is a pure power-law $(t/\tau_0)^a$, as found in the trap model [12] or standard coarsening models. This solution is particular in the sense that (15) is then *independent* of the microscopic time scale τ_0, which can be taken to zero; in this case C_A simply depends on the ratio t/t_w (full aging situation, a qualitative approximation of the experimental results, as explained in Sect. 2.1).

[5] This technical difficulty is related to the introduction of a time re-parametrization invariance when studying the *exact* mean-field equations for large and widely separated times t_w and $t + t_w$.

This is not the case for more general functional forms. Two explicit choices which have been proposed so far are:

$$h(t) = \exp\left[\frac{1}{1-\mu}\left(\frac{t}{\tau_0}\right)^{1-\mu}\right] \qquad \text{or} \qquad h(t) = \exp\left[\ln^a(t/\tau_0)\right] \ . \tag{17}$$

The form on the left was proposed to account for experiments in polymer glasses by Struik [23], then used in the first accurate analyses of aging effects in the TRM-decay [3, 28], and recently found in the exact solution of the asymmetric spherical SK model with $\mu = 1/2$ [47] (see also [38]). The second form is suggested by the numerical data from the "toy model" of a point particle in a random potential with infinite dimension [39]. Both will be used below to scale the data for the TRM and the out-of-phase susceptibility. Note that in the limit $\mu = 1$ or $a = 1$, one recovers full aging with a pure power-law behavior for h, while $\mu = 0$ corresponds to time translation invariance (no aging). When $\mu < 1$ and $a > 1$ we have "sub-aging" that we define as follows. Taking t fixed and, say, in the beginning of the aging regime, $h(t_w)/h(t + t_w) \sim 1 - (d\ln(h(t_w))/dt_w)t$. This defines a characteristic relaxation time $\tau(t_w)$. We say that we have sub-aging (super-aging) when $\tau(t_w)$ grows slower (faster) than t_w.
Interestingly enough, one can in general derive a relation between α, $(1-x)$ and X (see (14), (16) and (13) for their definitions) [39, 45]:

$$X\frac{(\Gamma[1+(1-x)])^2}{\Gamma[1+2(1-x)]} = \frac{(\Gamma[1-\alpha])^2}{\Gamma[1-2\alpha]} \ , \tag{18}$$

for single scale models. We shall use this equation to predict X at the beginning of the beginning of the aging regime in Sect. 4.2.

– On the other hand, there are models such as SK that have an infinite number of time-scales - correlation scales - apart form the stationary one [42, 15, 38]; mathematically, one has ultrametricity in time for all correlations such that $C_A < q_{EA}$, in the sense that $C_A(t_1, t_3) = \min(C_A(t_1, t_2), C_A(t_2, t_3))$, $t_1 > t_2 > t_3$ [15]. The decay is here infinitely slower than in the single-scale models. The FDT-violating factor $X[C_A]$ is a nontrivial function of C_A. These models are solved by a *full replica-symmetry breaking* ansatz when using the replica trick at the static level [4], and can be called "multi-scale" models.

It is important to notice that a scaling like (15) inside a correlation scale and ultrametricity between different correlation scales are expected to hold on very general grounds, in particular for more realistic finite dimensional models (in the limit of large-times), *provided that* the rather mild assumptions used in [14, 15] are satisfied. This justifies the fact that we shall use, in the following, a scaling-law like (15) to scale the data for real spin glasses, without refering to any particular model.

Connection with Measurable Quantities. If linear response theory holds, the TRM is just

$$M(t+t_w,t_w) = h\int_0^{t_w} ds\, R(t+t_w,s)\ . \tag{19}$$

For large waiting-time t_w, this integral can be rewritten using the decomposition in stationary and non-stationary decays ((10) and (13)) and using (14), for $t \gg \tau_0$ we have

$$\frac{M(t+t_w,t_w)}{M_{fc}(t+tw)} - A\left(\frac{\tau_0}{t}\right)^{\alpha} \propto \int_0^{C_A} dC'_A\ X[C'_A]\ . \tag{20}$$

where A is a constant. For single scale models as in (15) the scaling reads

$$\frac{M(t+t_w,t_w)}{M_{fc}(t+tw)} - A\left(\frac{\tau_0}{t}\right)^{\alpha} \propto \jmath^{-1}\left(\frac{h(t_w)}{h(t+t_w)}\right)\ . \tag{21}$$

In the early epochs of the aging regime for the TRM, that should be compared to the non-stationary behavior of the $\chi''(\omega,t)$, one has

$$\frac{M(t+t_w,t_w)}{M_{fc}(t+tw)} - A\left(\frac{\tau_0}{t}\right)^{\alpha} \propto q_{EA} - c\left(1-\frac{h(t_w)}{h(t+t_w)}\right)^{1-x}\ , \tag{22}$$

where we used (16).

The out-of-phase susceptibility can also be simply related to the correlation function (5). For high-frequencies, $\omega t \to \infty$, the aging term does not contribute (it is the integral of a slowly varying function $R_A(t,s)$ times a rapidly oscillating function). Using (14) to approximate the remaining integral, one finds the stationary part of the a.c. susceptibility:

$$\chi''(\omega,t) \to \chi''_{eq}(\omega) \propto \omega^{\alpha}\ , \qquad \omega t \to \infty\ . \tag{23}$$

Conversely, if $\omega t \geq 1$, *i.e.* for low frequencies, the aging part strongly contributes. For single-scale models we then have

$$\chi''(\omega,t) - \chi''_{eq}(\omega) \sim \frac{X}{T} h\omega \int_0^t ds \exp(i\omega s)\ \jmath^{-1}\left(\frac{h(s)}{h(t)}\right)\ , \qquad \omega t \geq 1\ . \tag{24}$$

For ωt finite but large, one has in general:

$$\chi''(\omega,t) - \chi''_{eq}(\omega) \propto \jmath^{-1}(1) - \jmath^{-1}\left(1-\frac{1}{\omega t}\,\frac{d\ln h(t)}{d\ln t}\right) \tag{25}$$

$$\propto \left(\frac{d\ln h(t)}{d\ln t}\,\frac{1}{\omega t}\right)^{1-x} \qquad 1 \ll \omega t < \infty\ , \tag{26}$$

where we introduced the power-law behavior of $\jmath^{-1}(u)$ in the vicinity of $u=1$ defined in (16). Hence the conclusions for χ":

- If $h(t)$ is a simple power-law, then $\chi''(\omega,t)-\chi''_{eq}(\omega)$ scales as ωt, as obtained in [12, 13] (full aging).
- If $h(t)=\exp(1/(1-\mu)t^{1-\mu})$ then $\chi''(\omega,t)-\chi''_{eq}(\omega)$ is a function of $\omega t \times (t/\tau_o)^{\mu-1}$. When $\mu \neq 1$ there is a correction to the pure ωt scaling (sub-aging for $\mu<1$)).
- If $h(t)$ is of the form $\exp[\ln^a(t/\tau_0)]$, then the ωt scaling is corrected by a slowly varying factor $\ln^{(a-1)}(t/\tau_0)$ (sub-aging if $a>1$). The χ" data are scaled within this assumption in the inset of Fig.2.

In Sect. 4, we apply the scaling relation (15) from single-scale models together with these proposals for $h(t)$ to the TRM and χ'' data.

The mean-field models which lead to the above results are very instructive: general statements and new ideas (like the violation of FDT) have emerged from their study. However, the physical mechanism underlying aging in these models is not yet very clear. The single-scale models, in particular, are very weakly sensitive to temperature, suggesting that no activated effects are involved, and that aging is rather related to large dimensional effects: the system wanders indefinitely in a large phase-space, without ever reaching a local minimum of the free energy [21]. Conversely, the trap model which we shall discuss now relies on activated effects to generate a broad distribution of time scales, which also leads to aging. However, this model is phenomenological, and does not emerge from a precise microscopic description - although some steps in this direction have recently been made [22, 48]. A tentative classification of the different models of aging has been proposed in [49].

3.3 The Trap Model

In the trap model [12], aging has been shown to naturally occur in a situation called "weak ergodicity breaking", which corresponds here to a statistical impossibility for the system to realize equilibrium occupation rates of the metastable states. This model has appeared as a fertile guideline for the analysis of the experiments; we therefore recall its main points, and come back to it later in Sect. 5.2. In the simplest version of the model [12], aging is sketched by a random walk in a collection of "traps" with random trapping times τ, all equally accessible. To each trap is associated a certain magnetization M and ac susceptibility $\chi_\tau(\omega)$. The properties of a real sample are obtained by averaging over an ensemble of decorrelated *subsystems*, corresponding to spins in different regions of space [6]. An important input is common to microscopic theories [4], and also to the more general problem of manifolds in random media [22, 48]; the distribution of trap

[6] At this stage, the spins do not enter directly. In later developments [26], however, the number of spins to be flipped for escaping from a trap (and hence the size of the subsystems referred to above) has been estimated from the influence of the field amplitude on the dynamics, as observed in the experiments.

depths is taken as an exponential. For thermally activated processes, this yields the following distribution of trapping times:

$$\psi(\tau) = \frac{x\tau_0^x}{\tau^{1+x}} \quad (\text{for } \tau \gg \tau_0) \quad , \tag{27}$$

where x (from the distribution of barrier heights) is a temperature dependent parameter describing the structure of the phase space. In a comparable way, the "random energy model" (REM) of Derrida [50] involves $x = T/T_g$. The crucial point is that $x < 1$ in the spin-glass phase; in consequence, the mean value of $\psi(\tau)$ is divergent, that is the mean time needed to explore the whole set of traps (and thus to reach ergodicity) is infinite. This was called weak ergodicity breaking, in the sense that the equilibrium situation is never realized, although the system never gets trapped in a finite region, leading to an asymptotically zero correlation function – see (8). This is very different of the usual ergodicity breaking, where the system can reach rather quickly an equilibrium configuration, but remains in a restricted sector of the phase space. Since $x < 1$, the distribution (27) is very broad. After a random walk during t_w, the system has visited numerous short-life traps, but in a relatively small time compared with t_w; as usual with such broad distributions, the significant contributions arise from the largest - although rare - events. Thus, after t_w, the system has the largest probability to be found in a trap of characteristic time t_w itself; if a magnetic field is varied at t_w, most subsystems will need a time of order t_w before changing their magnetization. It has been shown [12] that the TRM-decay is then a function of t/t_w, and similarly that the ac susceptibility is a function of $\omega.t$. Thus, on the basis of a statistical description in the space of the metastable states, the main features of aging can be obtained. Further developments of this approach [13, 52] are discussed below at the light of various aspects of the experimental results. We now turn to a more detailed description of the combination of aging *and* stationary dynamics as seen in *both* TRM and χ" measurements.

4 TRM Experiments: Aging and Non-Aging Dynamics Disentangled

4.1 Departures from Full t/t_w Aging

In Fig.1.b, the TRM curves are presented as a function of t/t_w; it is clear that this is not exactly the correct reduced variable (failure of a full aging scaling). The same effect has been found in other samples [3, 28] and can be seen in results from other laboratories (*e.g.* [1]). It has been first identified in polymer mechanics [23]. Indeed, the χ" results recall us that stationary dynamics, namely

$\chi"_{eq}(\omega) \propto \omega^{\alpha}$ (an additive contribution to the aging part, see Fig. 2), must intervene in the TRM decay, particularly in the $t \ll t_w$ regime. This frequency-dependent $\chi"_{eq}(\omega)$ is equivalent to an additive contribution of the form $t^{-\alpha}$ to the TRM.

The question of the departure from full aging has already been discussed in the past and the TRM's have been very accurately parametrized as the *product* of a $t^{-\alpha}$ factor times a (t, t_w) dependent factor ([28], see also the footnote[2] above). However, an additive combination of the stationary and aging parts arises naturally in the above theoretical approaches [14, 12], and we shall reanalyze these data in this light. We express the stationary part of the TRM, in units of the field-cooled value M_{fc} like in Fig. 1, as $A(\tau_0/t)^{\alpha}$. τ_0 is again a microscopic time, which allows homogeneity of the units, and then A is a non-dimensional constant, expected to be of order 1. We have taken the same TRM-data as in Fig. 1, and adjusted A and α in order to try to merge the aging parts $f(t_w, t)$

$$\frac{M}{M_{fc}} = A\left(\frac{\tau_0}{t}\right)^{\alpha} + f\left(\frac{t}{t_w}\right) \tag{28}$$

of all 5 curves of various t_w's as a function of t/t_w. We have no α values from $\chi"$-measurements on the $AgMn$ sample, so we have simply kept α in the $0.01 - 0.1$ range obtained for the $CdCr_{1.7}In_{0.3}S_4$ sample in previous analyses [28]. Fig. 3.a shows the result; whatever the choice of parameters (also, trying a logarithmic decrease instead of a power law), it seems impossible to merge all 5 curves together in the *whole time regime*. Systematic discrepancies are always found in the large t/t_w range: no simple function of t alone can account for these deviations. However, for small t/t_w, the good quality of the scaling *is equivalent* to the simple $\omega.t$-dependence of $\chi"(\omega, t)$, which is actually measured in the *same time regime* (*i.e.* $\omega t > 1$).

In the long time $t/t_w > 1$ region, the discrepancies shown in Fig. 3.a present the same features - although somewhat weaker - as in previous analyses using a multiplicative stationary contribution [28]. In Fig. 3.a, as well as in Fig. 1.b (the same, without stationary dynamics subtraction), it is clear that a t/t_w-scaling slightly overestimates the aging effect (sub-aging); the "youngest" curve (shortest t_w) lies *above* the others, whereas it was *below* in the raw data (Fig. 1.a), and the effect is sytematic for the 5 curves.

4.2 Sub-Aging Scaling

A way to succeed in merging all TRM curves is to use a generalized scaling function of the form $h(t) = \exp[\frac{1}{1-\mu}(\frac{t}{\tau_0})^{1-\mu}]$ with $\mu < 1$ (one of both examples quoted above in (17)). This was proposed in the context of spin glasses in [3, 28], as a phenomenological scaling procedure inspired from polymer mechanics [23], which proved to account with great accuracy for the observed sub-aging situation. We refer the reader to [3, 28] for the arguments which lead to the above choice of $h(t)$, or rather, along the lines of [28], to the *effective time* λ

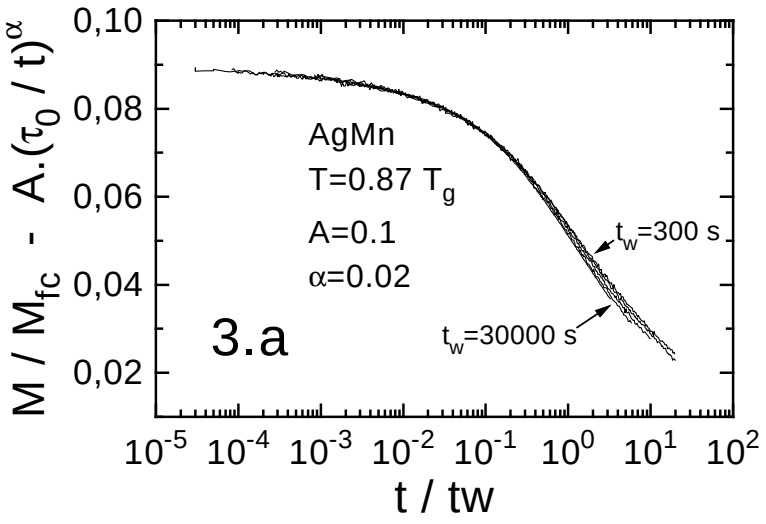

Fig. 3. a. Aging part of the TRM (Eq.28): the estimated stationary contribution has been subtracted from the full measured value. The data (same as in Fig. 1ab) is plotted *vs.* t/t_w.

defined as [7] :

$$\frac{h(t+t_w)}{h(t_w)} = \exp\frac{\lambda}{\tau_0} \quad . \tag{29}$$

As a function of λ, the 5 curves in Fig. 3.a recover precisely the same shape [3, 28], as displayed in Fig. 3.b. In other words, λ results from a change of variable which allows us to see the aging dynamics as *stationary*. It can also be obtained from

$$\frac{d\lambda}{\tau_0^\mu} = \frac{dt}{(t_w+t)^\mu} \quad , \tag{30}$$

which means that, since the age $t_w + t$ is varying during the TRM experiment, the effect of an elementary time interval dt depends on the elapsed time; due to sub-aging, the effective time scale associated to the age $(t_w + t)$ is $(t_w + t)^\mu$, with $\mu < 1$.

This type of scaling has been successfully applied to various samples [3, 28]; μ is found in the $0.8 - 0.9$ range and it is almost independent of temperature in the $0.3 < T/T_g < 0.9$ range. This μ-trick is a very convenient way of parametrizing the sub-aging deviations from a full t/t_w-scaling, although not necessarily having a direct physical meaning. $\mu = 0$ corresponds to the case of no t_w-dependence (no aging), while $\mu = 1$ would yield a full t/t_w scaling. The intermediate values

[7] The careful reader will notice a change of λ-units when compared with [28]; within the present definition, λ is equal to $\lambda(\frac{\tau_0}{t_w})^\mu$ from [28].

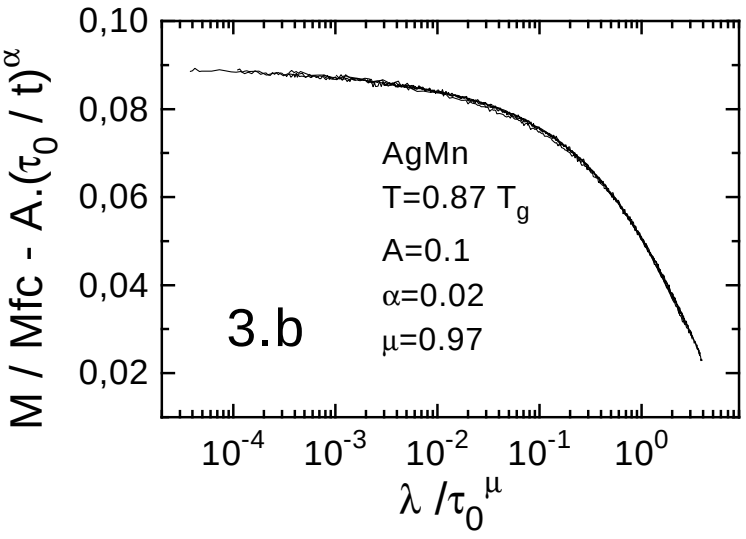

Fig. 3. b. Aging part of the TRM as in Fig. 3a, but *vs* the scaling variable λ/τ_o^μ defined in (29) (1st example in (17)). 5 curves, obtained for $t_w = 300, 1000, 3000, 10000, 30000s$ (same data as in Fig. 1 and 3a), are superimposed onto each other.

of μ (sub-aging) correspond to the fact that the apparent relaxation time scales sub-linearly (as $(t_w + t)^\mu$) with the age $t_w + t$.

The alternative choice of $h(t)$ proposed above in (17) can also be considered [53]. It is actually very close to the μ-case, in particular in the limit $\mu \to 1$. Again, for $a = 1$, full aging is recovered, while $a > 1$ describes a sub-aging situation, with an apparent relaxation time $\tau(t_w) = t_w/(a \ln^{(a-1)}(t/\tau_0))$. We have also applied this other sub-aging scaling to the non-stationary part of the relaxation displayed in Fig. 3a; the result is shown in Fig. 3.c, again the curves are fairly well superimposed onto each other.

Eq.(18), derived for single-scale mean-field spin-glass models, relates α, x and the FDT violating factor X defined in (13). According to (15) and (16), we have made a fit of the beginning of the TRM decay in Fig. 3.c (early epochs), and we have obtained $x \sim 0.96$ (see (16)). This is consistent with $X = 1$, which would suggest that FDT applies without corrections even at the beginning of the aging regime, if one accepts that (18) holds. This would be in accord with previous indications obtained through the comparison of χ'' and noise measurements made in the early epochs of the aging regime ("quasi-stationary regime") [28]. A careful and detailed study of the noise auto-correlation and response functions would help us knowing if and how FDT is violated, namely if X departs from 1 when going deeper in the aging regime. .

For the sake of comparison, we show in Fig. 3d how the μ-scaling applies to the full value of the TRM (the stationary contribution is neglected, and *not*

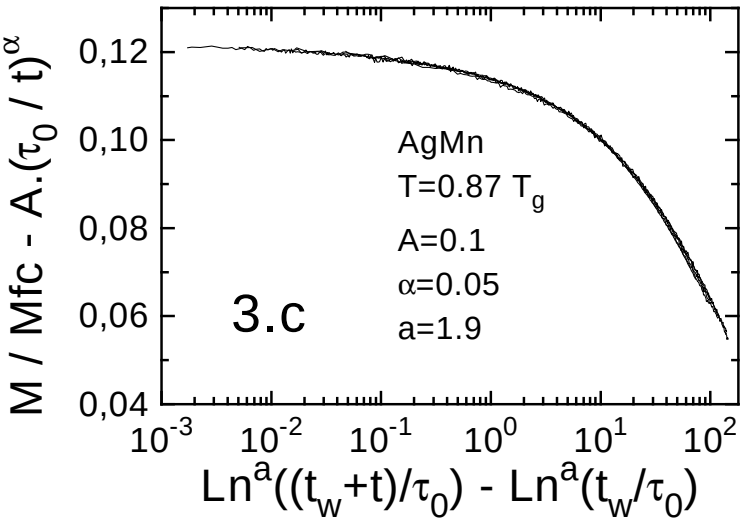

Fig. 3. c. Same as Fig. 3b, but as a function of a scaling variable which corresponds to the 2nd example in (17).

subtracted from the magnetization). An almost acceptable scaling is obtained; the discrepancies are not much larger than the experimental uncertainties, but *they are systematic*: all curves are crossing in the middle of the figure. This corresponds to $\mu = 0.87$. Neglecting the influence of the stationary contribution thus enhances the deviations from $\mu = 1$.

The very good scaling of the 5 curves in Figs. 3.b, 3.c, involves 3 free parameters: here $A = 0.1, \alpha = 0.02, \mu = 0.97$ or $A = 0.1, \alpha = 0.02, a = 2.2$. They correspond to a full account of the results, with good coherence between TRM and χ'' experiments. Let us summarize our points:

– The out-of-phase susceptibility $\chi"(\omega, t)$ is well represented by the sum of a stationary contribution, which varies like ω^{α} (or $(\ln \omega)^{power}$), plus a non-stationary contribution which varies as a negative power $x-1$ of $\omega.t$ (possibly with slowly varying corrections suggested by (26) above, but which are hardly visible on the χ'' data; see the rescaled χ" in the inset of Fig.2).

– The TRM decay curves are the sum of a stationary contribution $\propto t^{-\alpha}$, plus an aging contribution. In the time range ($t \ll t_w$) which is common to χ"-measurements, this aging part can be approximated (in agreement with χ") by a t/t_w-scaling. The long time regime $t \geq t_w$ seems however to prefer a sub-aging scaling of the type given in (17).

The origin of this weak ($1 - \mu = 0.03$) but insistant sub-aging behavior is an interesting point, still uncompletely understood. As mentionned above,

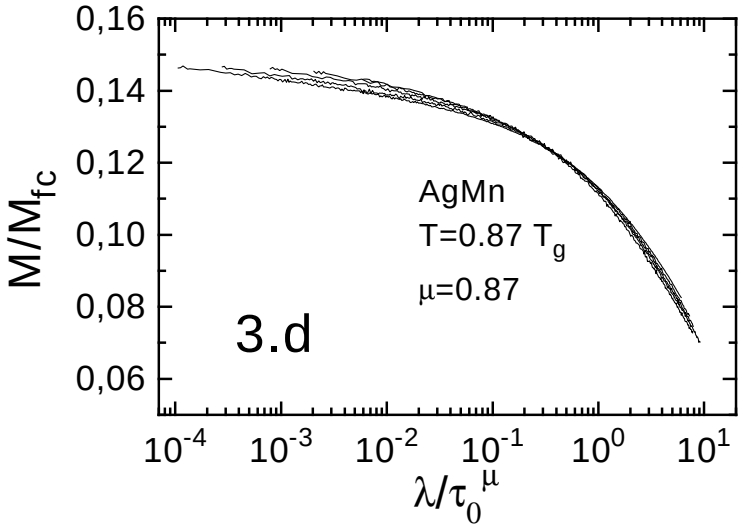

Fig. 3. d. Full measured value of the TRM (as in Fig. 1ab), but *vs* the scaling variable λ/τ_o^μ defined in (29).

from a theoretical point of view this would mean that the $\tau_0 \to 0$ limit of the underlying model does not exist. From a more physical point of view, several scenarios which might explain this effect can be considered. The simplest one concerns the effect of the field amplitude, which indeed (for larger fields) is known to suppress progressively the t_w-effect [8](see [26] for details). However, the parameter μ seems to stick to a plateau value (< 1) for the explored low-field range of $10 - 0.1Oe$ (systematic scaling analysis with *additive* (rather than multiplicative) stationary corrections are however needed to confirm this point).

This sub-aging behavior might also be interpreted as a sign that aging is actually "interrupted" beyond very long, but finite, times [52]. For example, if the trapping time distribution is cut-off beyond a certain ergodic time t_{erg} (which itself depends on the subsystem), then *for part of the subsystems* ergodicity will be realized within the time of the measurement: their dynamics will no more depend on t_w (interrupted aging). As shown in [52], this produces an effective sub-aging scaling very close to the $\mu < 1$ effect described here. The result is a value of a typical time t_{erg}, which must be understood as a *crossover time scale*, beyond which μ will further decrease to 0. In the analysis of [52], however, we had not properly taken into account the stationary contribution, which we have shown here to bring μ much closer to 1 (Figs. 3.b and 3.d). We had found t_{erg} of the order of $10^{6-7}sec$, which might therefore be underestimated.

[8] In a similar way, μ is seen to decrease with the stress amplitude in polymer glasses [23]

5 Towards a Hierarchical Description of the Space of the Metastable States

5.1 Temperature Variation Experiments

Main Qualitative Features: ac Measurements. Until now, we have only presented results which are obtained from aging experiments *at constant temperature* after the quench into the spin-glass phase. In another class of experiments, the temperature is varied during aging. In terms of thermally activated processes in a mountaneous free-energy landscape, one may expect to explore in more detail the various scales of the free-energy barriers which are involved in the slow dynamics. Thermal activation should - at first sight - be able to speed up or slow down the aging evolution. The conclusions of these experiments have been surprisingly instructive.

An early result was obtained in [54]; measuring the aging relaxation of χ" in a CuMn spin glass, the authors observed that any step increase or decrease in temperature was causing an instantaneous increase of χ", followed by a slow decrease. We may call this effect "restart of aging", since the relaxation is renewed by the temperature change, which hereby produces a similar effect as obtained after the quench. This phenomenon reveals that the slow aging evolution towards equilibrium is significantly disturbed by relatively small temperature changes. Such a "chaotic dependence" of the equilibrium states on temperature has been predicted to occur as a consequence of frustration in [56], where it is argued that the relatively small free-energy of an overturned region of spins (droplet) results from large cancellations at the surface of the droplet. These cancellations should be very sensitive to temperature, hence the strong effect of a small temperature variation.

When studied in more detail, the temperature variation experiments do not simply show a restart of aging upon *any* temperature change. We present in Fig. 4 an experiment performed in such a way that the reaction of the χ"-relaxation to either a *decrease* or an *increase* in temperature is very different [16]. The sample is first quenched from above $T_g = 16.7\ K$ to 12 K; due to aging, χ" slowly relaxes. After 350 min, the temperature is decreased to 10 K. Despite the reduced thermal energy, the relaxation does not slow down, but restarts abruptly from a higher value, in agreement with [54]; this is the surprising chaotic-like effect, which looks as if the system was (at least partially) restarting aging from the quench. But, when after another 350 min at 10 K the sample is heated back to 12 K, the result is very different: χ" resumes its slow relaxation from the value which had been reached before the temperature variation (see the inset of Fig. 4), in a *memory-like* effect.

There is no contradiction with the results in [54]. The experimental conditions of Fig. 4 are chosen here as the most illustrative of this twofold effect. Indeed, for smaller temperature variations, more intricate situations can be found [55]; aging at the lower temperature may partly contribute to aging at the higher temperature, even with a temporary incoherent transient, as emphasized *e.g.* in [17]. What we want to stress here is that a restart of aging is always observed

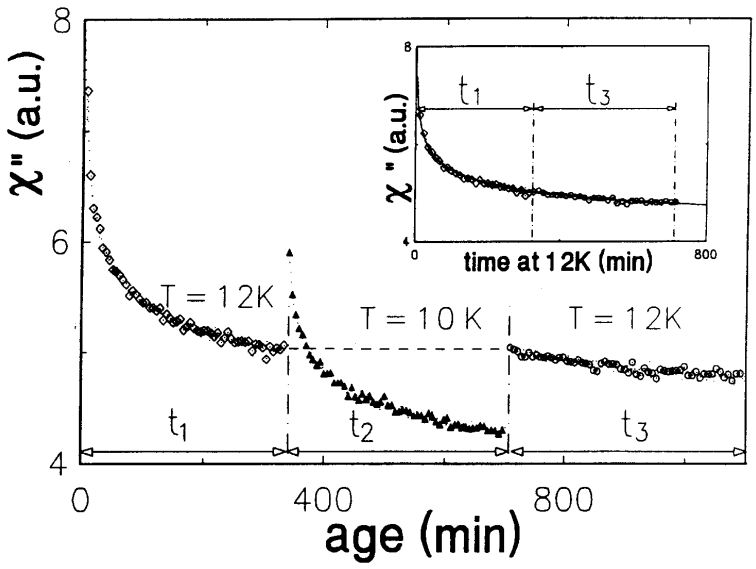

Fig. 4. Out of phase susceptibility $\chi''(\omega, t_a)$ of the $CdCr_{1.7}In_{0.3}S_4$ sample ($T_g = 16.7K$) during a temperature cycle. The frequency ω is 0.01 Hz, and t_a is the time elapsed from the quench. The inset shows that, despite the strong relaxation at 10 K, both parts at 12 K are in continuation of each other.

after a temperature decrease; in contrast, what is found upon a temperature increase is a memory of previous aging *at this higher temperature*. On the one hand, if a long time has been spent previously at the higher temperature, as is the case in Fig. 4, only a weak relaxation is found; on the other hand, if the system has been *directly* quenched to a given temperature, heating up afterwards to a higher temperature - for which no memory of previous aging exists - will produce a strong relaxation at this temperature (see examples of various situations in [55]).

Same Effects in TRM Experiments. The effect is quantitatively confirmed by measurements of the TRM-relaxation [25, 16]. The comparison with χ" requires some care; the χ"-relaxation directly shows *on-line* aging as a function of time, whereas in the TRM the effect of aging during t_w is considered *afterwards*, during the relaxation which follows the field cut-off at t_w. The TRM curve shows the relaxation processes in a wide time window, and thus yields more extensive information than χ" at a given frequency ω (which mainly reflects the processes of characteristic time $\simeq 1/\omega$). In Fig. 5.a, a negative temperature cycling has been applied during the waiting time.

From the above χ" results, one expects that aging processes be restarted

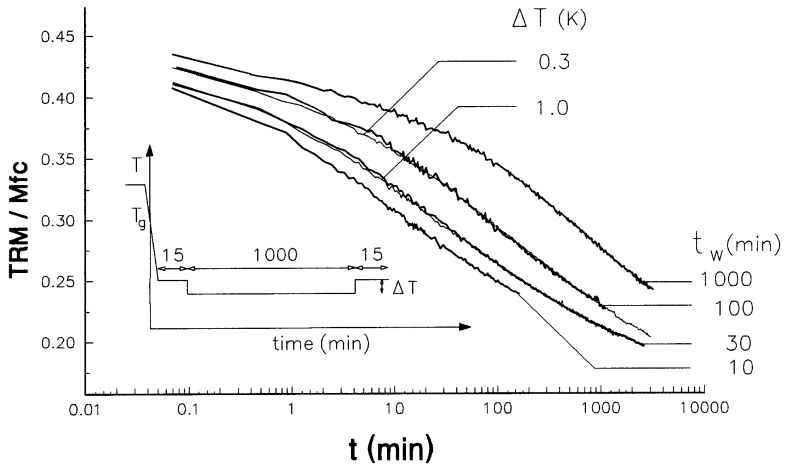

Fig. 5. a. Effect on the TRM relaxation of a *negative* temperature cycle ($CdCr_{1.7}In_{0.3}S_4$ sample, $T_g = 16.7K$). After waiting $t_{w+} = 15min$ at T_0 ($= 12K = 0.7T_g$), the sample is cooled to $T_0 - \Delta T$ for $t_{w-} = 1000min$, and then is heated back to T_0; after another $t_{w+} = 15min$, the field is cut and the relaxation measured (at T_0). These relaxations (thin lines) are compared with normal ones, measured after waiting $t_w = 10, 30, 100 or 1000min$ at constant T_0 (bold lines).

when going to $T_0 - \Delta T$; but for sufficiently large ΔT this evolution will be erased when coming back to T_0. This is what can be checked in Fig. 5.a for $\Delta T = 1K$: the procedure yields a relaxation curve which is exactly superimposed onto that obtained after simply waiting $t_{w+} + t_{w+} = 30min$ at constant T_0, aging during $t_{w-} = 1000min$ at 11 K has not contributed. Note that the equivalent normal curve has $t_w = 30min = 2t_{w+}$, not $15min$ (see Fig. 5a); the memory of the first aging stage has indeed been preserved.

Intermediate ΔT values produce intermediate situations; for $\Delta T = 0.3K$, the resulting curve is the same as that obtained after waiting $t_{eff} = 100min$ at constant T_0. From this example, we can work out a quantitative discussion of the effect. If we consider that the same characteristic free-energy barrier has been crossed by thermal activation during

i) $t_{w+} + t_{eff} + t_{w+} = 100min$ at T_0 and

ii) (t_{w+} at T_0) + (t_{w-} at $T_0 - \Delta T$) + (t_{w+} at T_0),

then we can write

$$(T_0 - \Delta T) \ln \frac{t_{w-}}{\tau_0} = T_0 \ln \frac{t_{eff}}{\tau_0} \quad , \tag{31}$$

which yields for the attempt time τ_0 the unpleasant value of $\sim 10^{-42} s$. Obviously, the *memory effect* cannot be explained by the only thermal slowing down of

jumping processes over constant height barriers.

In addition, simple thermal effects cannot be expected to explain the restart of aging, which is again evidenced in the positive cycling procedure of Fig. 5.b (all temperatures remain below T_g).

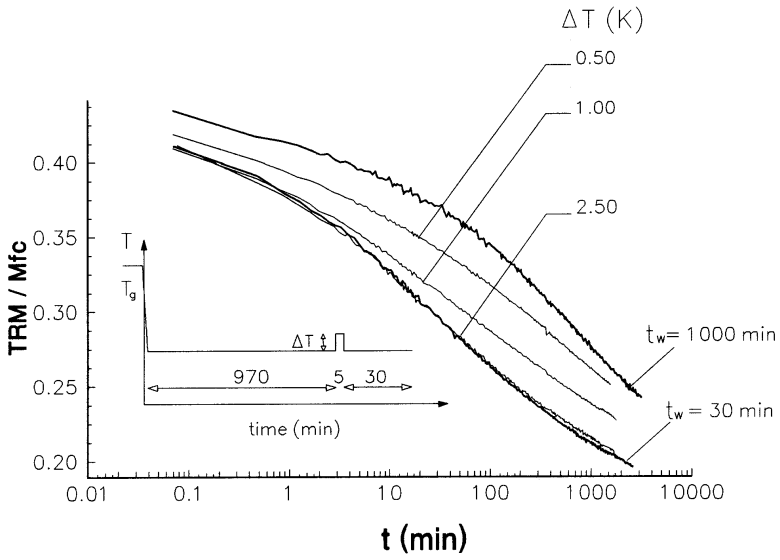

Fig. 5. b. Effect on the TRM relaxation of a *positive* temperature cycle ($CdCr_{1.7}In_{0.3}S_4$ sample, $T_g = 16.7K$). A short heating cycle is applied after 970 min of waiting time at T_0; then one still waits 30 min before cutting the field and measuring the relaxation at T_0 (thin lines). These relaxations are compared with normal ones, measured after waiting $t_w = 30$ *or* $1000min$ at constant T_0 (bold lines).

What appears in this procedure is the restart of aging due to the temperature decrease at the end of the cycle; for a sufficient ΔT ($= 2.5K$), the restart is so strong that the 970 min of previous aging are completely erased, as proved by the superposition of the $\Delta T = 2.5K$ curve with a normal $t_w = 30min$ one.

Again, for intermediate ΔT values, the effect is only partial; in its short-time part, the $\Delta T = 1K$ curve sticks to the young $t_w = 30min$-curve, whereas in its long-time part it goes closer to older ones. In contrast with the result in Fig. 5.a (negative T-cycling), the present procedure (positive T-cycling) yields curves which are not equivalent to a given waiting time at constant temperature. Clearly, the reason for that is that the positive temperature cycle ends by cooling down to T_0 (which produces a partial restart of aging at T_0), whereas the negative temperature cycle ends by heating back to T_0 (which lets the system retrieve the memory of the previous aging at T_0).

Thus, the same features of aging are observed in χ" and TRM experiments [16, 25]. A chaotic nature [56] of the spin-glass phase appears when the temperature is decreased, the restart of aging processes being very similar to what initially happens after the quench. On the other hand, a memory effect is found when the temperature is raised back, and this memory effect goes far beyond what can be expected from thermal slowing down.

A Hierarchical sketch. These effects have been interpreted in terms of a *hierarchical organization* of the metastable states as a function of temperature [25, 16]. The empirical picture is sketched in Fig. 6.

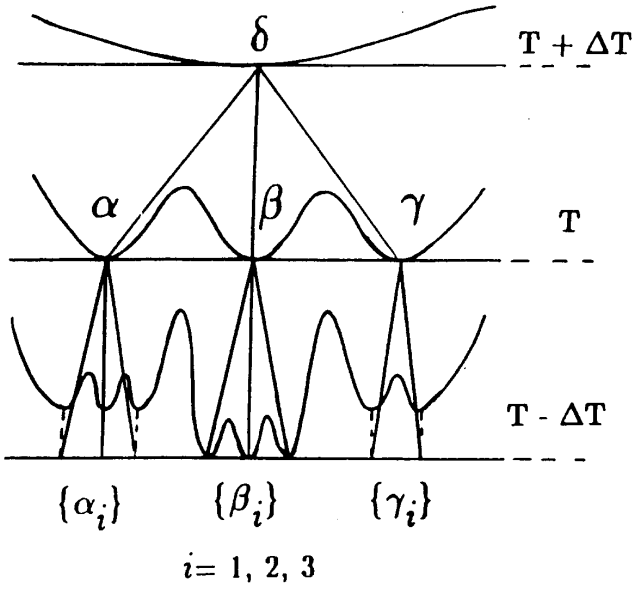

Fig. 6. Schematic picture of the hierarchical structure of the metastable states as a function of temperature.

During aging at a given T, the system samples the free-energy valleys (metastables states) at a given level of a hierarchical tree; the restart of aging upon lowering the temperature is figured out as a subdvision of the free-energy valleys into others, pictured as the nodes of a lower level of the tree, which thus develops multifurcating branches as the temperature decreases. The system is partially quenched since it must now search for equilibrium in a new, unexplored landscape, therefore aging (at least partially) restarts. The hierarchical picture

naturally provides us with the observed memory effect; when the temperature is raised back, the newly born valleys and barriers merge back to the previous free-energy landscape. Thus, aging at $T - \Delta T$ may have *not contributed* to the evolution at T, as far as all subvalleys which could be explored at $T - \Delta T$ originate from unique valleys of the landscape at T (which is realized for large enough ΔT).

The interpretation of these effects in a picture where aging is seen as the growth of *compact*, independent domains (droplets [6], domains [7]) remains, in our opinion, difficult [9] . The droplets may be broken into smaller ones when the temperature is decreased, thus producing a restart of aging; but the memory effect implies that some information is kept somewhere about the *stage of aging which had been reached before decreasing the temperature*. Thus, large-scale correlations should be kept untouched, while on the other hand they should apparently be destroyed. A way to satisfy these requirements could be to consider that the droplets should be fractal (non space filling) [8, 51], with a non trivial internal structure, in such a way that large droplets may contain smaller ones which can be activated independently. These droplets inside droplets might lead, under some energetic conditions, to a space-transcription of the hierarchical organization of the states.

More Quantitatively: Rapid Growth of Free-Energy Barriers. The observed effect on aging of various thermal histories is in contradiction with thermal activation over *constant height* barriers, as evidenced above in (31). The picture can be made more quantitative along this same line (Fig. 5.a and 31), which we now further develop. In one experiment, the spin glass is aged during t_w^- at $T - \Delta T$, and brought back to T before cutting the field and measuring the relaxation. In another experiment, the spin glass is simply aged during t_w^0 at T, and the relaxation is measured at T. If both decay curves are the same in the whole time window, we may consider that the aging states reached in both procedures are the same, and that equivalent regions of both landscapes at $T - \Delta T$ and T have been explored. We can characterize each evolution by a typical height B of the maximum barrier which has been crossed in each case, namely

$$B(T - \Delta T) = (T - \Delta T).\ln \frac{t_w^-}{\tau_0} \tag{32}$$

$$B(T) = T.\ln \frac{t_w^0}{\tau_0} \quad . \tag{33}$$

Thanks to the identity of the TRM curves obtained in each procedure, one may consider that this quantifies the T-variation of the *same barrier*, which limits in both cases the *same region* of the phase space. The contradiction pointed out in (31) shows that $B(T - \Delta T) > B(T)$; in other words, the hierarchical picture of valleys bifurcating into valleys as the temperature decreases is supported by the observation of the growth of free-energy barriers.

[9] See [25, 16]. However, some experiments have been analyzed along this line, with the introduction of long-time effects for the breakup of the domains [7, 17].

An extensive series of TRM measurements on the AgMn sample, for multiple values of t_w^-, T and ΔT, has been performed [18]. In brief, the result is that the barriers are growing for decreasing temperatures below T_g, and in addition that their growth rate is so fast that *at any* $T < T_g$ some of them should even *diverge* (see details in [18]). This provides us with an interesting link to the Parisi solution of the mean-field spin glass [4]. For decreasing temperatures, some barriers separating the metastable states are diverging, transforming the valleys into pure states in the sense of the Parisi solution; the hierarchical structure of the valleys, deduced from the experiments, can thus be related to that of the pure states. Also, the picture which emerges from these results is that of a *critical regime* at any $T < T_g$; in a sequence of micro-phase transitions starting at T_g, the spin-glass phase space continuously splits into nested and mutually inaccessible regions, within which non trivial dynamics takes place.

5.2 Aging as a Random Walk: Traps on a Tree

From a One-Level to a Multi-Level Tree. In its first stage [12], the trap model deals with all-connected traps, which can be called a "one-level tree" (see Sect. 3.3). The basic quantity which is calculated is the spin-spin correlation function $C_A(t_w + t, t_w)$, which can be related to the relaxation function if the fluctuation-dissipation theorem holds (in non-equilibrium, generalized forms of FDT might nevertheless hold [14], see Sect. 3.2). The aging part M_A of the TRM-relaxation can thus be estimated from the decay of the aging correlation function, which is proportional (by a factor q_{EA}) to the probability $\Pi(t, t_w)$ that the system has not jumped out of a t_w-trap at $t_w + t$:

$$M_A(t + t_w, t_w) \sim C_A(t_w + t, t_w) = q_{EA}.\Pi(t, t_w) \quad . \tag{34}$$

The probability Π contains all the information on possible jumps from trap to trap, and thus represents the aging dynamics; it should tend to 1 when t_w goes to infinity, for any finite t. In this limit, equilibrium dynamics is recovered, since no jump occurs; the proportionality factor q_{EA} in (34) describes this "bottom of the traps" dynamics (*cf.* with (14) in Sect.3.2). From its definition, it represents the overlap between the various configurations which constitute the bottom of the traps; in a TRM experiment, it is this finite fraction of the initial magnetization which should be found in the ideal limit of infinite t_w.

Two asymptotic behaviors of $\Pi(t, t_w)$ (and thus of the TRM) are calculated in a "multi-level" version of the trap model [13]:

$$\begin{aligned} t \ll t_w \qquad & \Pi(t, t_w) \sim A - \left(\frac{t}{t + t_w}\right)^{1-x_M} \\ t \gg t_w \qquad & \Pi(t, t_w) \sim \left(\frac{t}{t + t_w}\right)^{x_1} \quad , \end{aligned} \tag{35}$$

The predicted shape of the aging TRM is thus a constant minus a power law of exponent $1 - x_M$ for the short times ($t \ll t_w$), and on the other hand

a simple power law of exponent x_1 at long times ($t \gg t_w$). In the simple one-level case of all-connected traps with trapping times distributed with a given x (27), one has $x_1 = x_M = x$, which does not yield a realistic TRM-decay shape. However, a satisfactory fit to the TRM measurements can be obtained with only two values of x [13, 52]; one finds from the initial part of the TRM (or from χ'' measurements) $x_M \sim 0.65 - 0.8$ and from its late part $x_1 = 0.05 - 0.35$ (for several samples and different temperatures). In Fig.7, we show the asymptotic behaviors corresponding to (35) for a typical TRM curve, $1-x_M$ being equivalent to the exponent in (22) if $h(t)$ is a power law.

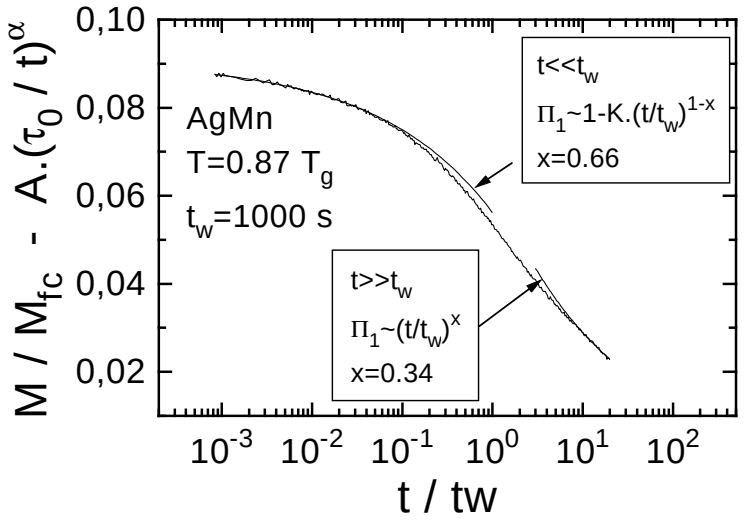

Fig. 7. Aging part of one of the above TRM curves (Fig. 1 and 3). Both asymptotic limits $t \ll t_w$ and $t \gg t_w$ have been fitted to (35). The variation of the effective index x along the different time regimes suggests a more complex than one-level tree structure.

Thus, if one thinks in terms of a one-level picture with no further assumption, it appears from the shape of the TRM itself that the effective x which labels the trapping time distribution (27) is *different* in the short and long-time regimes. Namely, x is closer to 1 for $t \ll t_w$ ($x = x_M$), and decreases for $t \gg t_w$ ($x = x_1$). This simple observation has been translated in terms of a hierarchical organization of the traps (traps inside traps); the model of all-connected traps [12] (one-level tree) has thus been generalized in [13], of which we now extract the main points.

The one-level tree is a distribution of traps of index say $x = x_1$ (< 1); following the construction of the Parisi tree of states [4], it can be extended into an n-level tree by multifurcating each trap into others of index $x_2 > x_1$, which themselves subdivide into others, until some final index $x_n > 1$ at the

end-branches of the tree. At each level i, the x_i-distribution of trapping times corresponds [4, 12] to an x_i-dependent distribution of free energies, and this yields for the overlap between the corresponding states a value $q_i(x_i)$ which is the inverse of the Parisi order parameter $q(x)$ [4], thus $q_{i+1} > q_i$. Now, the states close to the end-branches (say the lower part of the tree) with $x > 1$ can all be visited in finite times, since for $x > 1$ the mean value of the distribution (27) is finite: the corresponding dynamics is *stationary*.

Aging phenomena appear when $x < 1$, i.e. above a given level c such that $x_c = 1$. The faster processes of the aging regime, which are seen in the short-time part of the TRM, occur among the states which are close to each other in the hierarchical geometry (large overlap), that is which are related by a tree-node at a level very cloes to c; therefore they correspond to x close to 1, as is indeed suggested by the exponent of the power law behavior at the beginning of the TRM. As time elapses, more distant states (of smaller overlap) can be explored, and the corresponding transitions imply passing higher nodes in the tree, of smaller index x, in agreement with the smaller exponent of the power law in the long-time part of the TRM.

The model can be solved for an arbitrary number of levels; but the simpler case of a *two-level* tree has been computed and fitted to the TRM experiments [13]. The fits are of a very good quality for both insulating and metallic samples: for a given t_w, the shape of the decay curve is quite well reproduced over the whole t scale. If the number of metastable states at each level is infinite, however, the predicted influence of t_w is precisely a t/t_w scaling (full aging), as in [12], and this does not satisfactorily account for the measured t_w-dependence, which corresponds to a sub-aging behavior (see the discussion in Sect. 4).

Effect of Temperature Changes. Now, the effect of the temperature on this tree-like organization of the metastable states can also be discussed. From the fit of the TRM-data [52], the x_M-index (e.g. from the short-time part) shows a tendency to increase towards 1 as T approaches T_g; this suggests that the spin-glass transition be closer to the REM scenario [50], where $x = T/T_g$, than to the mean-field equilibrium scenario [4] where the Parisi parameter x rather goes to zero at T_g. This leads us to a possible interpretation of the empirical *hierarchical structure versus temperature* in terms of the Parisi-like tree of traps [13].

T_g is characterized by a certain c-level of the tree where $x_c = 1$; the temperature dependence of x means that, when the temperature is lowered, this is now a lower (multifurcated) level of the tree which corresponds to $x = 1$ and limits the stationary dynamics. Thus, aging dynamics restarts among newly born states, as observed in the experiments and interpreted along the hierarchical scheme of Fig. 6. Conversely, when the temperature is raised back, the lower aging level comes back to equilibrium, and aging continues at the upper level, resuming from its previous stage of evolution. A more detailed comparison between theory and experiment is however desirable. Note finally that a hierarchical decoupling of time scales has also been argued on the basis of "second" noise spectra by Weissman

and collaborators [58].

The influence of temperature is thus crucial in these pictures where activated processes play the dominant part in aging. Conversely, temperature is somewhat irrelevant for the aging dynamics of the mean-field models described above (at least those corresponding to single-scale dynamics). For example, the effect of temperature variations has been explicitely computed within the spherical $p = 2$ model [57], with the result that nothing comparable to experiments happens. In this respect, aging in these single scale models is again very similar to simple domain growth in a ferromagnet [21], which is rather insensitive to temperature. It would be very interesting to understand how temperature changes affect the dynamics of a multiscale model, such as the SK model.

6 Conclusions

In this paper, we have presented a survey of the experimental results concerning aging phenomena in spin glasses, focusing on the description of magnetization relaxation and low-frequency out-of-phase susceptibility measurements. We have discussed in some details how far two theoretical approaches of out-of-equilibrium effects, namely the trap model [12, 13, 52] and the microscopic approach [14, 15], can succeed in describing different aspects of the dynamics.

The relaxation of the out-of-phase susceptibility χ" towards a non-zero value indicates the presence of stationary dynamics. This same dynamics can be found, although less obviously, in the short-time part (compared to the waiting time t_w) of the decay of the thermo-remanent magnetization (TRM). In fact, an additive combination of a stationary and an aging regime in the auto-correlation (and thus also in the TRM and in χ") follows from the solution of some mean-field models [14, 15, 38, 39, 57]. This striking similarity of mean-field and real spin glasses raises the question of the nature of the slow dynamics in these systems. While one is used to think of thermal activation in mountaneous landscapes as the source of slow processes, the mean-field models now provide us with aging phenomena which are due to the flatness of large regions in the phase space [21], with no crucial role played by the temperature.

For the sake of a coherent description of both TRM *and* χ" data, one should therefore extract the same stationary contribution from all results, which we have made here in an additive way. The remaining *aging contribution* presents, for the TRM, systematic departures from a "full aging" situation of a pure t/t_w scaling ("sub-aging") [3, 28]. When the stationary dynamics of the TRM is additively accounted for, the departures from full aging become less pronounced, but still remain. For χ", whose aging regime only overlaps that of the TRM on a limited range, both full aging and sub-aging scalings remain compatible with the

data. Using some recent analytical developments of the microscopic approach of spin-glass dynamics [15], we have shown that a sub-aging behavior will appear under some general conditions. Thus, the microscopic theory can now account for the scaling functions which had been postulated in the past by the experimentalists on phenomenological grounds [3, 28].

The experiments have shown that small temperature variations have a strong effect on aging phenomena [16, 17, 18]. A temperature decrease restarts the evolution, whereas raising back the temperature lets the system retrieve its previous stage of aging at this same temperature. These results have been interpreted in terms of a hierarchical organization of the metastable states as a function of temperature, in which the valleys of the free-energy landscape subdivide into others for decreasing temperatures [16, 18]. The mean-field models have not yet brought conclusive results on this question. The trap model [12], which provides us with a stochastic picture of aging, has recently been extended [13] in a way which sheds some light on the temperature variation experiments.

The simple picture of a random walk among all-connected traps (one-level tree of states) did not take into account the existence of stationary dynamics, which in this language is a "bottom-of-the-traps" dynamics. For this reason, traps must have an internal structure. On the other hand, the TRM shape is related to the index x of the trapping time distribution. The comparison of the experimental shapes with a one-level tree model shows that the "effective x" systematically varies along the curve; it is closer to 1 in the $t \ll t_w$ regime, and smaller in the $t \gg t_w$ regime [12, 52, 13]. Thus, the traps which are explored in the various time regimes are not connected in the same way.

These results are fairly well understood within a picture of hierarchically connected traps, in a multi-level tree geometry where x varies from one level to the other. The limit value $x = 1$ sets the tree level which is at the border of stationary and non-stationary dynamics. The tendency of x to increase when the temperature approaches T_g [52] indicates that this border $x = 1$ level changes with temperature; the resulting model of a tree-like organization where the limit of equilibrium dynamics changes with temperature [13] is now very close to the empirical picture of a hierarchy of metastable states as a function of temperature which had been drawn from the experiments [16].

This recent development, together with the predictions of slow dynamics and aging from microscopic models, have created a very stimulating atmosphere. They let us expect that an even tighter interaction among theoreticians and experimentalists will bring us closer to a more complete understanding of the physics of disordered systems.

Acknowledgements We would like to thank L. Balents, D. Dean, Vik. Dotsenko, M. Feigel'man, J. Kurchan, P. Le Doussal, M. Mézard, R. Orbach and G. Parisi for numerous stimulating discussions all along this work.

References

1. L. Lundgren, P. Svedlindh, P. Nordblad and O. Beckman; Phys. Rev. Lett. **51** 911 (1983).
2. R.V. Chamberlin; Phys. Rev. **B30**, 5393 (1984).
3. M. Ocio, M. Alba and J. Hammann; J. Physique Lett. (France) **46**, L-1101 (1985).
   M. Alba, M. Ocio and J. Hammann; Europhys. Lett. **2**, 45 (1986).
4. K. Binder and P. Young; Rev. Mod. Phys. **58**, 801 (1986).
   M. Mézard, G. Parisi and M. A. Virasoro; *Spin Glass Theory and Beyond*. World Scientific Lecture Notes in Physics Vol **9** (Singapore, 1987).
   K. Fischer and J. Hertz; *Spin Glasses*, (Cambridge University Press, 1991).
5. A. J. Bray and M. A. Moore; J. Phys. **C17**, L463 (1984), in Heidelberg Coll. in Glassy Dynamics, Springer-Verlag, 1986.
6. D. S. Fisher and D. Huse; Phys. Rev. **B38**, 373 (1988).
7. G. Koper and H. Hilhorst; J. Phys. France **49**, 429 (1988).
8. M. Ocio, J. Hammann and E. Vincent; J. Magn. Magn. Mat. **90-91**, 329 (1990).
9. Vik. Dotsenko, M. Feigel'man and Ioffe; *Spin Glasses and Related Problems*, Soviet Scientific Reviews **15**, (Harwood, 1990).
10. H. Hoffmann and P. Sibani; Phys. Rev. **A38**, 4261 (1988).
11. H. Hoffmann and P. Sibani; Phys. Rev. Lett. **63**, 2853 (1989); Z. Phys. **B80**, 429 (1990).
12. J-P Bouchaud; J. Phys. I (France) **2**, 1705 (1992).
13. J.P. Bouchaud and D.S. Dean; J. Phys. I (France) **5** (1995) 265.
14. L. F. Cugliandolo and J. Kurchan; Phys Rev. Lett. **71**, 173 (1993); Phil. Mag. **71**, 501 (1995).
15. L. F. Cugliandolo and J. Kurchan; J. Phys. **A27**, 5749 (1994).
16. Ph. Refregier, E. Vincent, J. Hammann and M. Ocio; J. Phys. (France) **48**, 1533 (1987).
    F. Lefloch, J. Hammann, M. Ocio and E. Vincent; Europhysics Lett. **18**, 647 (1992).
17. P. Grandberg, L. Sandlung, P. Nordblad, P. Svendlindh, L. Lundgren; Phys. Rev. **B38**, 7097 (1988).
18. M. Lederman, R. Orbach, J. M. Hammann, M. Ocio and E. Vincent; Phys. Rev. **B44**, 7403 (1991).
    J. Hammann, M. Lederman, M. Ocio, R. Orbach and E. Vincent; Physica **A185**, 278 (1992).
19. C. A. Angell; Science, **267**, 1924 (1995). C. A. Angell, P. H. Poole and J. Shao; Il Nuovo Cimento **16**, 993 (1994).
20. Y.G. Joh, R. Orbach and J. Hammann; submitted to Phys. Rev. Lett. (This paper proposes a model for the time dependence of TRM and ZFC magnetization based on the same hierarchical picture as in Sect. 5.1, and a linear increase of the barrier heights with the Hamming distance).
21. J. Kurchan and L. Laloux; J. Phys. **A29**, 1929 (1996).
22. J.P. Bouchaud and M. Mézard, in this volume.

23. L. C. E. Struik; *Physical Aging in Amorphous Polymers and Other Materials*, Elsevier, Houston (1978).
24. P. Nordblad, L. Lundgren and L. Sandlund; J. Magn. Magn. Mat. **54**, 185 (1986).
25. E. Vincent, J. Hammann and M. Ocio; in *Recent Progress in Random Magnets* p.207-236, editor D.H. Ryan, World Scient. Pub. Co. Pte. Ltd., Singapore 1992.
26. E. Vincent, J-P Bouchaud, D. S. Dean and J. Hammann; Phys Rev **B52**, 1050 (1995).
27. D. Chu, G.G. Kenning and R. Orbach; Philos. Mag. **B71**, 489 (1995).
28. M. Alba, J. Hammann, M. ocio and Ph. Refregier; J. Appl. Phys. **61**, 3683 (1987).
    Ph. Refregier, M. Ocio, J. Hammann and E. Vincent; J. Appl. Phys. **63**, 4343 (1988).
    J. Hammann, M. Ocio and E. Vincent; ; in *Relaxation in Complex Systems and Related Topics* p.11-21,edited by I.A. Campbell and C. Giovanella, Plenum Press, New-York 1990.
29. see e.g.: J. Souletie and J.L. Tholence; Phys. Rev. **32**, 516 (1985),
    H. Bouchiat; J. Physique (France) **47**, 71 (1986),
    E. Vincent and J. Hammann; J. Phys. **C20**, 2659 (1987),
    and references therein.
30. S. Edwards and P. W. Anderson; J. Phys. **F5**, 965 (1975).
31. see, *e.g.*, P. W. Anderson and C. M. Pond; Phys. Rev. Lett. **40**, 903 (1978).
    J. A. Hertz, L. Fleshmann and P. W. Anderson; Phys. Rev. Lett. **43**, 943 (1979).
    E. Marinari, G. Parisi and F. Ritort; J. Phys. **A27**, 2687 (1994).
    N. Kawashima and A. P. Young; Phys. Rev. **B53**, R484 (1996).
32. D. Sherrington and S. Kirkpatrick; Phys. Rev. Lett. **35**, 1792 (1975).
33. J. O. Andersson, J. Mattson and P. Svedlindh; Phys. Rev. **B46**, 8297 (1992); *ibid* **B49**, 1120 (1994).
34. H. Rieger; J. Phys. **A26**, L615 (1993); J. Phys. **I** (France), 883 (1994); Annual Rev. of Comp. Phys **II**, 295 (1995).
35. L. F. Cugliandolo, J. Kurchan and F. Ritort; Phys. Rev. **B49**, 6331 (1994).
36. H. Yoshino; J. Phys. **A29**, 1421 (1996).
37. G. Parisi, F. Ricci and J. Ruiz-Lorenzo; cond-mat/9606051.
38. S. Franz and M. Mézard; Europhys. Lett. **26**, 209 (1994); Physica **A209**, 1 (1994).
39. L. F. Cugliandolo and P. Le Doussal; Phys. Rev. **E53**, 1525 (1996).
    L. F. Cugliandolo, J. Kurchan and P. Le Doussal; Phys. Rev. Lett. **76**, 2390 (1996), and in preparation.
40. A. Crisanti, H. Horner and H-J Sommers; Z. Phys. **B92**, 257 (1993).
41. H. Kinzelbach and H. Horner; J. Phys. I (France) **3**, 1329 (1993), *ibid*, 1901 (1993).
42. H. Sompolinsky; Phys. Rev. Lett. **47**, 935 (1981).
43. H. Sompolinsky and A. Zippelius; Phys. Rev. **B25**, 6860 (1982).
    P Biscari; J. Phys. **A23**, 3861 (1990).
44. Th. Nieuwenhuizen; Phys. Rev Lett **74**, 4289 (1995), *ibid*, 4293.
45. J-P Bouchaud, L. F. Cugliandolo, J. Kurchan and M. Mézard; Physica **A226**, 243 (1996).
46. A. Crisanti and H-J Sommers; Z. Phys. **B87**, 341 (1992).
47. L. F. Cugliandolo, J. Kurchan, P. le Doussal and L. Peliti; cond-mat/9606060.

48. L. Balents, J-P Bouchaud and M. Mézard; cond-mat/9601137, J. Phys. **I** (France), to be published.
49. A. Barrat, R. Burioni and M. Mézard, J. Phys. **A29** (1996)1311.
50. B. Derrida; Phys. Rev. Lett. **45**, 79 (1980); Phys. Rev. **B24**, 2613 (1981).
51. A similar concept has been proposed by J. Villain in *Europhys. Lett.* **2** (1986) 871.
52. J.-P. Bouchaud, E. Vincent and J. Hammann; J. Phys. I (France) **4**, 139 (1994).
53. L. F. Cugliandolo and J. Kurchan; unpublished.
54. L. Lundgren, P. Svedlindh and O. Beckman, Journal of Magn. Magn. Mat. **31-34**, 1349 (1983).
55. E. Vincent, J-P Bouchaud, J. Hammann and F. Lefloch; Phil. Mag. **71**, 489 (1995).
56. D.S. Fisher and D.A. Huse; Phys. Rev. Lett. **56**, 1601 (1986). A.J. Bray and M.A. Moore; Phys. Rev. Lett. **58**, 57 (1987).
57. L. F. Cugliandolo and D. S. Dean; J. Phys. **A28**, 4213 (1995).
58. M. B. Weissmann, N.E. Isrealoff, G. B. Alers, Journal of Magn. Magn. Mat. **114**, 87 (1992).

This article was processed using the LaTeX macro package with LMAMULT style